Received: 12 June 2017 | Revised: 15 November 2017 | Accepted: 1 January 2018

DOI: 10.1002/sia.6394

RESEARCH ARTICLE

WILEY SURFACE and INTERFACE ANALYSIS

# Cathodoluminescence study of defects in thermal treatment of zinc titanate thin films deposited by a cosputtering process

Tun-Yuan Chiang[1] | Chien-Huang Tsai[2] | Ming-Chao Huang[3] | Hua-Chiang Wen[4] | Wu-Ching Chou[4]

[1] Department of Mechanical Engineering, Chin-Yi University of Technology, Taichung 400, Taiwan, ROC

[2] Department of Automation Engineering, Nan Kai University of Technology, Nantou 54243, Taiwan, ROC

[3] Department of Electrical and Information Technology, Nan Kai University of Technology, Nantou 54243, Taiwan, ROC

[4] Department of Electrophysics, National Chiao Tung University, Hsinchu 300, Taiwan, ROC

**Correspondence**
Chien-Huang Tsai, Department of Automation Engineering, Nan Kai University of Technology, Nantou 54243, Taiwan, ROC.
Email: chtsai12@gmail.com

**Funding information**
National Science Council of Taiwan, Grant/Award Numbers: 105-2221-E-252 -003 and MOST 104-2221-E-252 -007

The effects of thermal treatment of polycrystalline ZnO–$TiO_2$ systems on their luminescence emission and phase properties were investigated using ex situ cathodoluminescence and backscattering electron microscopy. The main features of the spectrum are a blue band at 2.75 eV for the phase of TiO and a complex visible band at 2.18 eV for the phase of ZnO, whose peak intensity depends on the annealing temperature. The spectrum intensity is dominated by the ZnO phase when annealing temperature was 720°C, which is attributed to abnormal grain growth. Competition is observed between the broad band peaked at 2.18 eV and visible band peaked at 2.75 eV as the annealing temperature changed (820°C-920°C). The cathodoluminescence density is gradually governed by the $TiO_2$ phase, and the emission in polychromatic and monochromatic imaging is stronger equally at 920°C. The nucleation of the $TiO_2$ and ZnO grains is present in the backscattering electron images as well.

**KEYWORDS**

backscattering electron microscopy, cathodoluminescence, radio frequency magnetron cosputtering

## 1 | INTRODUCTION

The ZnO–$TiO_2$ system has attracted considerable attention because of its many applications as an inorganic compound. Three compounds exist in the ZnO–$TiO_2$ system[1]: $Zn_2TiO_4$ (cubic), $ZnTiO_3$ (hexagonal), and $Zn_2Ti_3O_8$ (cubic). The electrical and chemical properties of the compounds in the ZnO–$TiO_2$ system make them attractive for a range of commercial applications, for example, white pigment, catalytic sorbent,[2-4] microwave dielectric materials,[5] gas sensors,[6] high performance catalysts,[7,8] and luminescent materials. $ZnTiO_3$ can be prepared by solid-state reaction, sol-gel,[9] bulk manufacture,[10] and chemical vapor deposition.[11] In recent years, Radio frequency (RF) sputtering has been applied to produce the stable state of pure $ZnTiO_3$ (hexagonal phase), which can exist after annealing between 700°C and 800°C. The crystalline phases $ZnTiO_3$ (hexagonal) and $TiO_2$ (rutile) could be coexisted at the annealing temperature of 600°C.[12] However, the decomposition from hexagonal $ZnTiO_3$ to cubic $Zn_2TiO_4$ and rutile $TiO_2$ occurs at 920°C.[13] Meanwhile, single-phase $Zn_2Ti_3O_8$ films were prepared at temperatures lower than the sintering temperature of the bulk specimen.[14] Earlier, we have concluded that the mechanical properties of the ZnO–$TiO_2$ system can be changed through its microstructures, grain sizes, and morphologies.[15,16] The real risks of this meta-stability in the ZnO–$TiO_2$ system to its applications has not yet been discussed in the literature. Markedly, the ZnO–$TiO_2$ system has attracted much attention for its optical properties. For example, ZnO–$TiO_2$ core-shell nanorods have improved UV photoresponse sensitivity.[17] Lin et al have found that based on the composite of ZnO nanorods and $TiO_2$, the band edge emission of ZnO nanorods can be enhanced up to 120 times.[18] For optoelectronic devices, doped ZnO films have also been deposited.[10,19-22] The properties of the ZnO–$TiO_2$ system that are responsible for the luminescence performance therefore becomes an interesting issue. Therefore, it is believed that the emission mechanism of ZnO–$TiO_2$ system needs to be evaluated using the cathodoluminescence (CL) technique. The CL spectra for $ZnTiO_3$ (hexagonal), $Zn_2Ti_3O_8$ (spinel), and $Zn_2TiO_4$ (cubic) prepared with different annealing temperature are acquired, and the emissions were studied in detail using CL mapping.

In this report, the author analyzed Zn–Ti–O films, where $ZnTiO_3$ was the phase, using the CL spectrum and CL mapping to improve the understanding of thermal treatment on the emission. In addition, backscattering electron (BSE) imaging was also used to observe the dominant Zn and Ti phases. Subsequently, the performance of the

  

resulting $ZnTiO_3$ films were examined as a function of the phases present and annealed.

## 2 | EXPERIMENTAL DETAILS

The $ZnTiO_3$ films were prepared using an RF magnetron cosputtering system using a 4-in-diameter sintered ceramic target (Zn and Ti). To deposit stoichiometric $ZnTiO_3$ films on the Si substrate, an $Ar–O_2$ flow (8:2) with a purity of 99.999% at a flow rate of 50 sccm was introduced into the chamber using mass flow controllers, and an RF power of 200 W was used. In addition, the sputtering pressure was $2 \times 10^{-2}$ Torr; the substrate temperature was set at 250°C; and the duration of the deposition was 1 hour. To remove the contaminants formed on the target surface and to stabilize the sputtering conditions, it was necessary for presputtering to be performed for 5 minutes prior to each deposition process. The specimens produced were subsequently subjected to ex situ thermal treatment at 720°C, 820°C, and 920°C in a furnace under $N_2$ gas for 2 hours using a heating rate of 5°C/min. The films were cs 220 nm in thickness. The detailed deposition conditions of the $ZnTiO_3$ films have been provided in previous articles.[15,16]

After deposition, the surface roughness and microstructure were analyzed using AFM (Veeco Dimension 5000, Scanning Probe Microscopy, D5000). Scanning electron microscopy (SEM) and BSE imaging (JEOL JSM-7001F, operated at 10 keV and 10 nA) were used to observe the surface morphology and elemental distribution, respectively. The effects of thermal-induced phase transformation on the luminescence properties of the $ZnTiO_3$ films were characterized at 300 K through CL spectroscopy and SEM (JEOL JSM-7001F, operated at 30 keV and 18 nA). The spot size of the electron beam was less than 10 nm under these conditions. The CL emissions were collected as polychromatic mapping and monochromatic mapping images.[23] The CL signals were measured using a Horiba Jobin-Yvon iHR550 0.5-m monochromator and detected by a liquid $N_2$-cooled charge coupled device with an energy resolution of 0.3 meV.

**TABLE 1** The RMS values of $ZnTiO_3$ with respect to the annealing temperatures

| $ZnTiO_3$ | RMS, nm |
|---|---|
| RT | 3.1 |
| 720°C | 6.2 |
| 820°C | 19.5 |
| 920°C | 21.6 |

## 3 | RESULTS AND DISCUSSION

Figure 1 shows the AFM images (5 × 5 μm) of the $ZnTiO_3$ films deposited on a silicon substrate. The surface roughness (RMS) increased with increasing annealing temperature, with roughness values of 3.1, 6.2, 19.5, and 21.6 nm for annealing temperatures of RT, 720°C, 820°C, and 920°C, respectively (Table 1). From our previous report,[15] a similar result was observed where the cavities were due to the evaporation of Zn, and the white particles were $TiO_2$ after thermal treatment. A trend was noted that the RMS increased with increasing annealing temperature: at 820°C, RMS = 19.5 nm, while at 920°C, RMS = 21.6 nm. Previous reports suggest that increasing the annealing temperature enhanced the atomic mobility and caused the film recovery to result in weak mechanical properties when the films are annealed under elevated temperatures.[15,16,19]

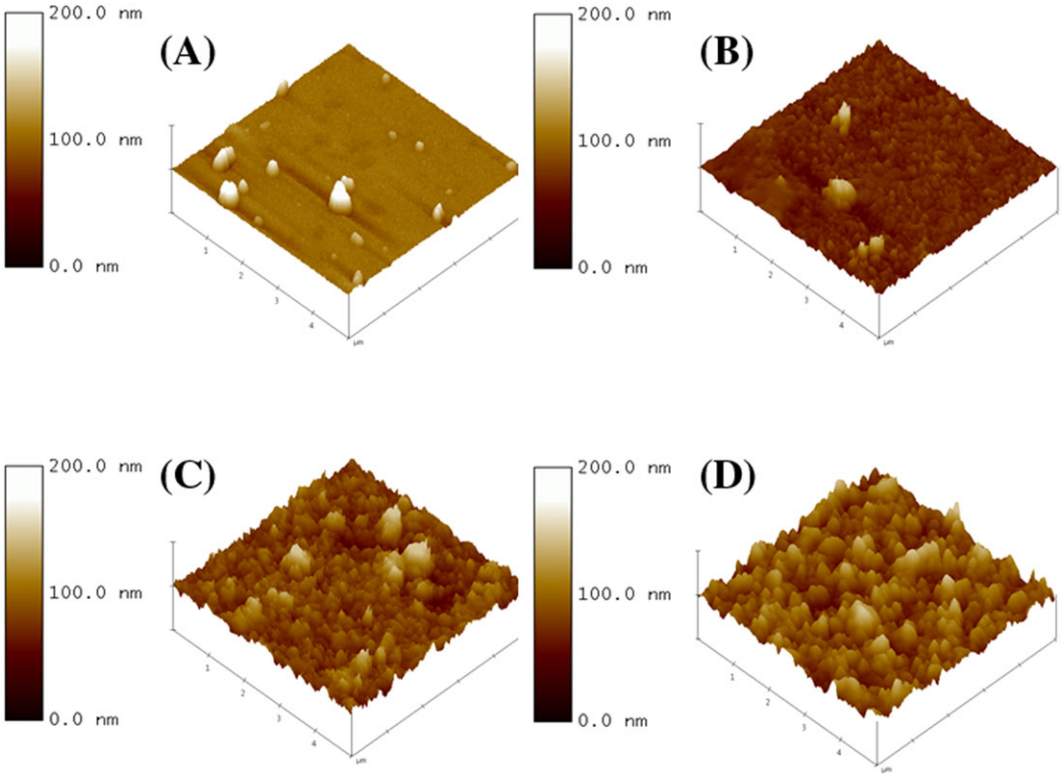


**FIGURE 1** 3 D-AFM images of the surfaces of $ZnTiO_3$ films after annealing: A, RT; B, 720°C; C, 820°C; and D, 920°C

Figure 2 shows SEM images of the specimens annealed at 720°C, 820°C, and 920°C. In the SEM and AFM images of those specimens, the particles have larger grain sizes and cover the surface more densely when the annealing temperature increases. The SEM images, CL mapping, and CL spectra are presented in Figure 2. In the specimen prepared without high temperature annealing, labeled RT, the film appears as a plane in the SEM (Figure 2A). The emission is shown in the CL spectrum (Figure 2D) of the RT specimen, which provides a low emission in the visible range and a broad band in the red spectral range centered at 1.9 eV (650 nm). The low emission maybe can be attributed to oxygen vacancy levels or interstitial oxygen defects.[15,16] Low brightness is obtained in both polychromatic imaging and monochromatic imaging (Figure 2B,C), which matched the trend of the response of the CL spectrum intensity. Particularly for the monochromatic surface image in Figure 2C, the emission at approximately 2.75 eV (450 nm) is quenched. Therefore, the brightness of the monochromatic image is darker than the polychromatic image (Figure 2B). The polychromatic image reveals that the inner film emits at 2.18 eV (569 nm) and 2.75 eV when annealed at 720°C (Figure 2F). For the specimen annealed at 720°C, the polychromatic image is brighter than the monochromatic image (Figure 2G). The CL spectrum of the annealed (720°C) specimen has a higher visible emission than the RT specimen. The CL spectrum consists of 2 bands that are centered at 2.18 and 2.75 eV (Figure 2H). In the recent work,[15,16] we found the

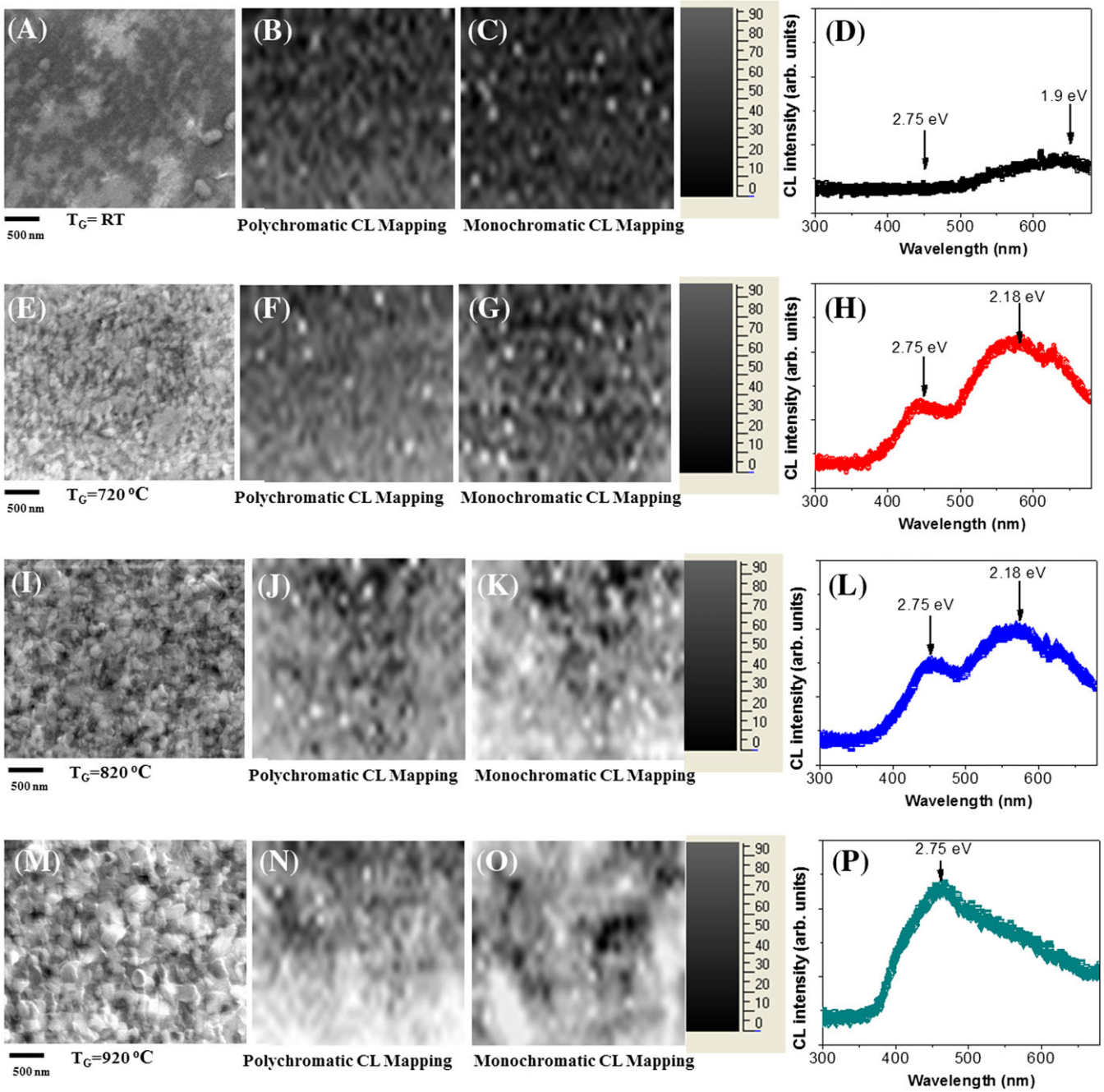


**FIGURE 2** Images of ZnTiO3 samples prepared at different annealing temperatures: RT with A, SEM; B, polychromatic CL mapping; C, monochromatic CL mapping; and D, CL spectrum; 720°C with E, SEM; F, polychromatic CL mapping; G, monochromatic CL mapping; and H, CL spectrum; 820°C with I, SEM; J, polychromatic CL mapping; K, monochromatic CL mapping; and L, CL spectrum; 920°C with M, SEM; N, polychromatic CL mapping; O, monochromatic CL mapping; and P, CL spectrum

increased intensity of the (104) orientation of $ZnTiO_3$ is obtained in the same samples. The preferred orientation tends to reduce its free energy to reach a stable state as well as to adjust chemical bonding states, which may be the reason for the higher emission efficiency. Many oxygen vacancies are transferred between Zn and Ti; $TiO_2$ traps electrons; and the shallow traps can act as radiative centers whose emission occurs around 2.75 eV.[24] In previous reports,[25] annealing sintered $TiO_2$ in oxygen at 800°C revealed that the centers of crystals are sensitive to oxygen, which agreed with the increased brightness of the monochromatic image of the annealed (720°C) specimen relative to the RT specimen. Otherwise, the brightness of the monochromatic image is still darker than polychromatic image, as shown in Figure 2 F-G. From the intensity of the CL spectrum (Figure 2H), we have observed that the emission intensity of ZnO (2.18 eV) and $TiO_2$ (2.75 eV) both increased compared to RT. The brightness of the polychromatic image is dominated by the phase of $TiO_2$ than that of the phase of ZnO when annealed at 720°C. The polychromatic image includes the emission intensity from the ZnO and $TiO_2$, which produces stronger emission than the monochromatic image ($TiO_2$ only). Comparing the images of the specimen annealed at 820°C, both the monochromatic and polychromatic images are very close in brightness intensity (Figure 2J,K). However, the intensity for the $TiO_2$ phase (2.75 eV) in the CL spectrum is increased (Figure 2L), and the intensity of the CL spectrum is higher than that for the film annealed at 720°C (Figure 2H). Hence, the $TiO_2$ is responsible for the increased emission in the monochromatic imaging when annealed at 820°C. The X-ray diffraction (XRD) patterns of the $ZnTiO_3$ films show that the (104), (110), (116), and (214) peaks of the hexagonal $ZnTiO_3$ phase were observed for the annealed (620°C) specimen.[12-16] For the annealed (820°C) specimen, the intensity of the (104) peak was higher, indicating that the film was highly oriented.[15] The preferred orientation tends to reduce its free energy to reach a stable state as well as to adjust chemical bonding states, which may be the reason for the enhanced emission efficiency at 820°C. The hexagonal $ZnTiO_3$ decomposes into cubic $Zn_2TiO_4$ and rutile $TiO_2$ at higher temperatures but the $ZnTiO_3$ phase remained stable when annealing temperature was 820°C.[26]

The RMS values increased (3.1~21.6 nm) with increasing annealing temperature (Table 1). We concluded that the grain size increased when annealing temperature reached 820°C, which causing many vacancies can diffuse more rapidly down boundaries leading to more newly grain boundaries are obtained due to the abnormal grain growth. However, the grain size increased when annealing temperature reached 920°C, which produced the boundaries are regions of high energy they make excellent sites for the nucleation of precipitates and other second- phases, eg, cubic $Zn_2TiO_4$ and rutile $TiO_2$ occur from hexagonal $ZnTiO_3$.[13] Ageh et al[27] have reported that the (104) planes of $ZnTiO_3$ coatings have extensive stacking faults bordered by partial dislocations, which serve as a pathway for dislocations to glide parallel to the sliding direction for the manner of high temperature solid lubrication. Sun et al[28] have discussed that the high stacking fault density (104) is present in $ZnTiO_3$ textured (104) planes, which provide friction-reducing surfaces/subsurfaces during interfacial sliding. This is the reason why the changes in the luminescence brightness among those samples are sensitive to the annealing temperature. The result of the CL mapping for a hexagonal symmetry is in good agreement with previous results.[15,16,27,28] Interestingly, when the same areas are examined, the emission in polychromatic and monochromatic imaging is stronger equally as the annealing temperature was 920°C (Figure 2 N,O). From the CL spectrum (Figure 2P), it is found that the intensity for the ZnO (2.18 eV) is lower than that for the $TiO_2$ (2.75 eV). The earlier XPS analysis showed that increased chemisorption of oxygen on metal produces a surface layer of adsorbed oxygen when the annealing temperature was 820~920°C.[15,16] It is suggested that the emission intensity in monochromatic imaging is governed by the quality of the films, which are preferentially related to the $TiO_2$ phase, for example, cubic $Zn_2TiO_4$ and rutile $TiO_2$.[12-16]

ZnO and $TiO_2$ phases are processed at high temperatures that end up with excessively large grain size (Table 1) and poor mechanical properties.[15] To evidence this problem, BSE analysis is often used to observe the grain growth. The SEM and the corresponding BSE images are presented in Figure 3. The $ZnTiO_3$ exhibits an increased polycrystalline morphology and a random distribution of particles when the annealing was performed. The BSE images show a dark and rough background with some bright particles scattered over the surface and located at the grain boundaries. Su et al have explored a grain boundary information of $Be_{0.4}Zn_{0.6}O$ films using BSE, and the results are comparable.[29] The cavities were not observed by SEM and BSE for the RT specimen because no evaporation of Zn occurred (Figure 3A, B). In a typical decomposition, the small second phases start to appear at the grain boundary (Figure 3C), which is a known step for annealed-induced nucleation. Thus, these bright spots appear to be the $TiO_2$ dominant phase. Further evidence is provided by the BSE image in Figure 3D. In a BSE configuration, the number of electrons elastically scattered from a phase increases with the increasing atomic number of that phase. Therefore, heavier atoms produce a greater scattering probability. It is noteworthy that some bright spots in the SEM image turn dark in the corresponding BSE images (Figure 3E,F), suggesting that they are composed of elements with a lower atomic number than Zn. The atomic number of Ti (22) is smaller than that of Zn (30); therefore, these darker spots in the BSE image are a Zn-rich phase. The BSE observations matched the trend of the RMS values when the annealing temperature was increased. As the film was annealed at 920°C, the areas consisted of Zn-rich (dark) and Ti-rich grains (light in the BSE image) (Figure 3G,H). This morphology demonstrated a truly mixed Zn and Ti oxide phase, where both types of oxides were distributed randomly since the Zn-rich grains are partially merged with the Ti-rich grains. However, the ZnTiO3 film has a weak (110) diffraction peak in the XRD pattern when annealed at 820°C. The preferred orientation tends to reduce its free energy to reach a stable state.[15,16] The trends seen in the earlier XPS and XRD studies provide further evidence that increased oxygen content creates the oxygen-rich regions that are preferentially formed in the $TiO_2$ phase.[12-14]

In closing, we have analyzed the $ZnTiO_3$ films, where $TiO_2$ was using CL technique to improve the understanding of thermal treatment on the emission.[30] Noted that, the $ZnTiO_3$ films have been compared to correlate the localization of the excitonic luminescence and the phase between of the ZnO and $TiO_2$. The visible band (2.75 eV) could be assigned to excitons bound to grain boundaries in a typical decomposition, which is the reason why strongly CL intensity appear to be the $TiO_2$ dominant phase.

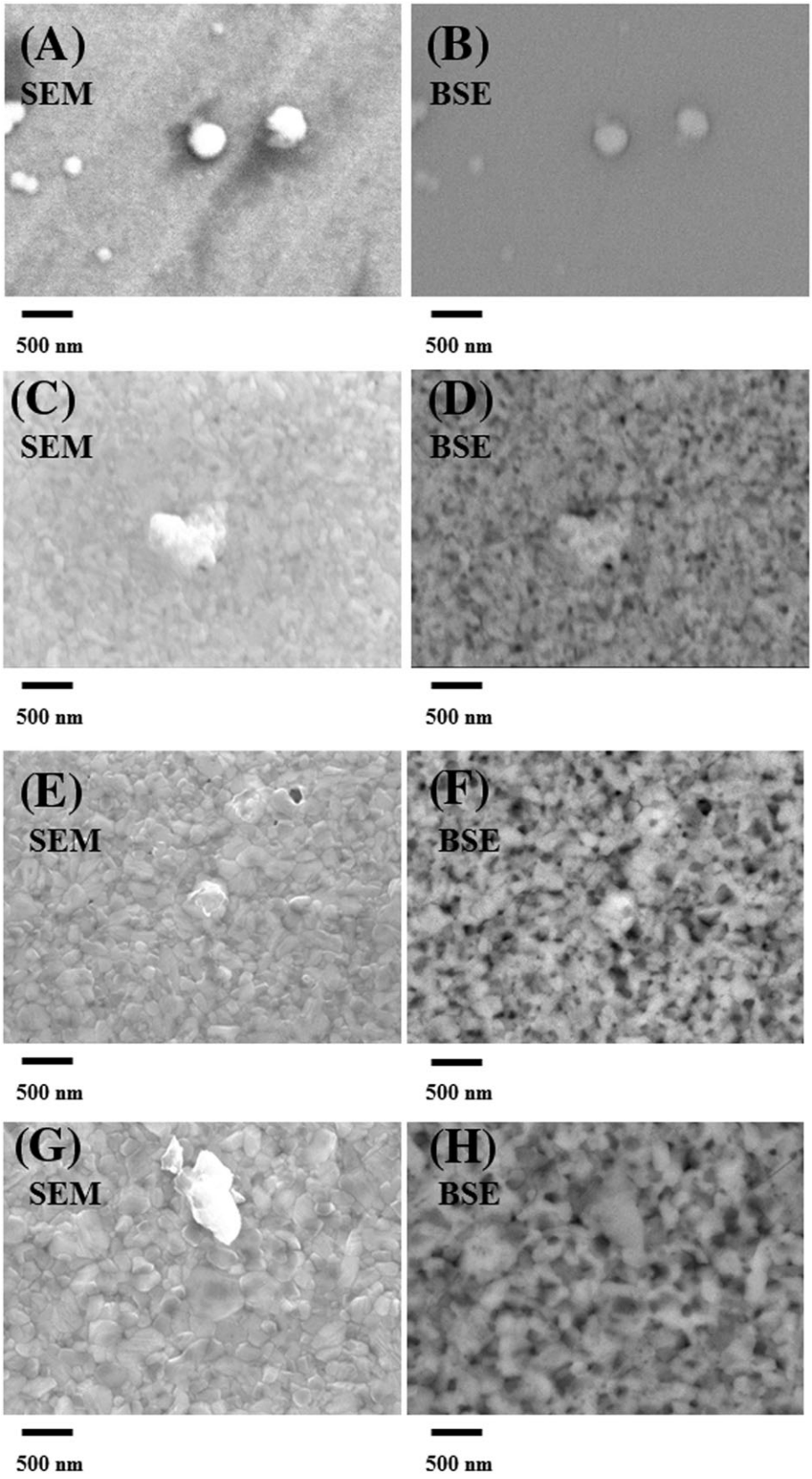


**FIGURE 3** SEM and BSE images of $ZnTiO_3$ thin films treated by conventional annealing conditions: A,B, RT; C,D 720°C; E,F, 820°C; and G,H, 920°C

## 4 | CONCLUSION

We have characterized RF magnetron cosputtered $ZnTiO_3$ films using AFM, CL spectrum, and CL mapping. The RMS values measured using AFM (5 × 5 μm) were 3.1, 6.2, 19.5, and 21.6 nm for annealing temperatures of RT, 720°C, 820°C, and 920°C, respectively. The CL spectra were also used to characterize the luminescence properties of the specimens. An enhanced emission is observed, and the emission

intensity is dominated by the abnormal grain growth and other second-phases, eg, cubic $Zn_2TiO_4$ and rutile $TiO_2$ occur from hexagonal $ZnTiO_3$ at 820~920°C. In addition, the emission might be associated with the increasing grain growth, which is comparable in their effect in poly-chromatic imaging and monochromatic imaging. Cathodoluminescence spectroscopy has been a very powerful tool for investigating sample quality under a variety of growth conditions. That is why we apply CL to confirm the effective trapping of the threading dislocation and the stacking fault of the samples.

The SEM and BSE observations match the trend of RMS from AFM. A small, regular particle with little grain growth is seen at RT. However, a distribution of grain sizes is produced as the annealing temperature is increased. From the BSE, observations can be seen that the surface was composed of a truly mixed and randomly distributed Zn and Ti oxide areas as well.

## ACKNOWLEDGEMENTS

This research was supported by the National Science Council of Taiwan under the MOST 104-2221-E-252 -007 and 105-2221-E-252 -003 contracts. The author thanks the Center for Advanced Instrumentation (Department of Electrophysics, National Chiao Tung University, Hsinchu 300, Taiwan, ROC) for assistance with the CL/SEM/EDS/BSE measurements (JEOL JSM-7001F field-emission scanning electron microscope) and Prof Y.R. Jeng for supporting the SPM equipment used in this study. We also thank Prof T.Y. Chiang, Dr Hua-Chiang Wen, and Prof Wu-Ching Chou for the help with the CL data analysis as well as the discussions.

## ORCID

*Chien-Huang Tsai* http://orcid.org/0000-0003-2204-1340

## REFERENCES

1. Dulin FH, Rase DE. Phase equilibria in the system ZnO-TiO2. *J Am Ceram Soc*. 1960;43(3):125-131.
2. Bartram SF, Slepetys RA. Compound formation and crystal structure in the system ZnO-TiO2. *J Am Ceram Soc*. 1961;44(10):493-499.
3. Labus N, Obradović N, Srećković T, Mitić V, Ristić MM. Influence of mechanical activation on synthesis of zinc metatitanate. *Sci Sinter*. 2005;37(2):115-122.
4. Wang SF, Lü MK, Gu F, et al. Photoluminescence characteristics of Pb2+ ion in sol–gel derived $ZnTiO_3$ nanocrystals. *Inorg Chem Commun*. 2003;6:185.
5. Kim HT. Microstructure and microwave dielectric properties of modified zinc titanates (I). *Mater Res Bull*. 1998;33(6):963-973.
6. Obayashi H, Sakurai Y, Gejo T. Perovskite-type oxides as ethanol sensors. *J Solid State Chem*. 1976;17(3):299-303.
7. Chen ZX, Derking A, Koot W, van Dijk MP. Dehydrogenation of isobutane over zinc titanate thin film catalysts. *J Catal*. 1996;161(2):730-741.
8. Yoon KH, Cho J, Kang DH. Physical and photoelectrochemical properties of the TiO2–ZnO system. *Mater Res Bull*. 1999;34(9):1451-1461.
9. Wang SF, Gu F, Lu MK, et al. Photoluminescence of sol-gel derived $ZnTiO_3$: Ni2+ Effect of nanocrystals. *Chem Phys Lett*. 2003;373(1-2):223-227.
10. Chang YS, Chang YH, Chen IG, Chen GJ, Chai YL. Synthesis and characterization of zinc titanate nano-crystal powders by sol–gel technique. *J Cryst Growth*. 2002;243(2):319-326.
11. Barreca D, Comini E, Ferrucci AP, et al. First example of ZnO–TiO2 nanocomposites by chemical vapor deposition: structure, morphology, composition, and gas sensing performances. *Chem Mater*. 2007;19(23):5642-5649.
12. Huang YL, Lee YC, Tsai DC, Shieu FS. Effect of annealing on formation and microstructure of ZnTiO3 thin films by dc reactive magnetron co-sputtering. *Mater Sci Forum*. 2011;687:610-616.
13. Lee YC, Huang YL, Lee WH, Shieu FS. Formation and transformation of ZnTiO3 prepared by sputtering process. *Thin Solid Films*. 2010;518(24):7366-7371.
14. Huang YL, Tsai DC, Lee YC, Jung DR, Shieu FS. Effect of annealing on microstructure and dielectric properties of $Zn_2Ti_3O_8$ thin films by reactive co-sputtering. *Surf. Sci Technol*. 2013;231:153.
15. Wu SC, Jeng YR, Yau WH, Wu KT, Tsai CH, Chou CP. Nanoindentation response of zinc titanate thin films deposited by co-sputtering process. *Appl Surf Sci*. 2012;258(18):6730-6734.
16. Wu SC, Yau WH, Tsai CH, Chou CP. Nanotribological behavior of thermal treatment of zinc titanate thin films. *Surf Interface Anal*. 2012;44(10):1314-1318.
17. Liang YC, Liao WK. Annealing induced solid-state structure dependent performance of ultraviolet photodetectors made from binary oxide-based nanocomposites. *RSC Adv*. 2014;4(37):19482.
18. Lin HY, Chou YY, Cheng CL, Chen YF. Giant enhancement of band edge emission based on $ZnO/TiO_2$ nanocomposites. *Opt Express*. 2007;15:13835.
19. Kong JZ, Zhou F, Wang Z, et al. Preparation and optical properties of high-quality oriented of Al and Er co-doped ZnO thin films. *J Sol-Gel Sci Technol*. 2012;63(1):95-102.
20. Chang YM, Lin ML, Lai TY, et al. Broadband omnidirectional light trapping in gold-decorated ZnO nanopillar arrays. *ACS Appl Mater Interfaces*. 2017;9(13):11985-11992.
21. Chiang TY, Dai CL. Enhancement of intrinsic emission from ultrathin ZnO films using Si nanopillar template. *Nanoscale Res Lett*. 2012;7,263.
22. Chiang TY, Dai CL, Lian DM. Influence of growth temperature on the optical and structural properties of ultrathin ZnO films. *J Alloys Compd*. 2011;509(18):5623-5626.
23. Wen HC, Chou WC, Yau WH, Fan WC, Lee L, Jian KF. Using nanoindentation and cathodoluminescence to investigate the residual stress of ZnSe. *J Alloys Compd*. 2015;625:52-56.
24. Fernández I, Cremades A, Piqueras J. Cathodoluminescence study of defects in deformed (110) and (100) surfaces of $TiO_2$ single crystals. *Semicond Sci Technol*. 2005;20:239.
25. Plugaru R, Cremades A, Piqueras J. The effect of annealing in different atmospheres on the luminescence of polycrystalline TiO2. *J Phys Condens Matter*. 2004;16(2):S261-S268.
26. Jung JS, Kim YH, Gil SK, Kang DH. Dielectric properties of zinc titanate thin films prepared by Rf magnetron sputtering. *J Electroceram*. 2009;23(2-4):272-276.
27. Ageh V, Mohseni H, Scharf TW. Processing–structure–tribological property interrelationships of zinc titanate coatings grown by atomic layer deposition. *Surf Coat Technol*. 2014;241:112-117.
28. Sun W, Ageh V, Mohseni H, Scharf TW. J. Du. *Appl Phys Lett*. 2014;104(24):241903.
29. Su L, Zhu Y, Chen M, et al. Temperature-dependent structural relaxation of BeZnO alloys. *Appl Phys Lett*. 2013;103(7):072104.
30. Wen HC, Chou WC, Chiang TY, Jeng YR, Fan WC. Using nanoindentation and cathodoluminescence to identify the bundled effect of gallium nitride grown by PA-MBE. *J Alloys Compd*. 2017;693:615-621.

**How to cite this article:** Chiang T-Y, Tsai C-H, Huang M-C, Wen H-C, Chou W-C. Cathodoluminescence study of defects in thermal treatment of zinc titanate thin films deposited by a cosputtering process. *Surf Interface Anal*. 2018;50:541–546. https://doi.org/10.1002/sia.6394